

# DOING THE MATHEMATICS OF FLUID FLOW NETWORKS

Mapundi Kondwani Banda  
10 October

Doing the mathematics of fluid flow networks

Inaugural lecture delivered on 10 October 2013

Prof M K Banda  
Applied Mathematics Division  
Department of Mathematical Sciences  
Faculty of Science  
Stellenbosch University

Editor: SU Language Centre

Printing: SUN MeDIA

ISBN: 978-0-7972-1459-0

Copyright © 2013 MK Banda



## ABOUT THE AUTHOR

Mapundi Kondwani Banda grew up in Malaŵi, where he completed his secondary school education at Bandawe Secondary School in 1986 and obtained a BSc degree from the University of Malaŵi in 1990. In 1991 he completed an MSc in Computing Science at the Imperial College of Science, Technology and Medicine, which was a constituent college of the then University of London. After developing an interest in Applied Mathematics and with a desire to see Mathematics being applied to real-world problems, he proceeded to do an MSc in Industrial Mathematics at the University of Kaiserslautern which he completed in 1997. In 2000 he enrolled for PhD research in the Numerical Methods

and Scientific Computing group led by Prof. A. Klar at the Darmstadt University of Technology which he completed in 2004. He was a postdoctoral fellow for a short term at the same university before returning to Malaŵi in 2004.

As a student, Mapundi received scholarships and awards which enabled him to study in London, Kaiserslautern and Darmstadt. He was a recipient of a scholarship from the Overseas Development Shared Scholarship Scheme (ODASSS) in 1990 and the German Academic Exchange Programme (DAAD) award in 1995 and in 1999.

In 1991, Mapundi was appointed as a Software Development Analyst at Business Computers Services Limited. He changed his career path to join academia at the University of Malaŵi, Chancellor College, as a lecturer in 1993. He was promoted to Senior Lecturer in 2004. He was appointed as a lecturer at the University of KwaZulu-Natal in 2005 and promoted to Senior Lecturer in 2008. In 2008 he joined the University of the Witwatersrand as an Associate Professor. In 2012 Mapundi moved to Stellenbosch to take a position as a Professor in the Applied Mathematics Division, Department of Mathematical Sciences, at Stellenbosch University.

He has been a research visitor at the following institutions: University of Kaiserslautern, RWTH-Aachen, Durham University, Tsinghua University and the University of British Columbia. He is a member of the editorial board of the SAMSA Journal of Pure and Applied Mathematics.



# Doing the mathematics of fluid flow networks

*Dedicated to all my students, teachers and collaborators*

## 1 Networked flow problems

In this address, I would like to present some of the experience that we have gained over the years since 2004 in the area of mathematical analysis of flows through domains which are interconnected by a network structure. One cannot help but think about examples like water supply networks, traffic flow through road networks, supply chain networks, blood flow networks, networks of exit corridors in a shopping mall as well as natural gas flow networks. The functionality of these networks is sometimes taken for granted but can it be proven to be foolproof? As a user of such systems one wishes that the system remains predictable and stable. In this address, gas flow networks will be used as a case study but in general the mathematical findings can be extended to other networks listed above and beyond. In general, it is sometimes difficult to identify deep and interesting mathematical problems in our everyday life experiences. As a secondary aim, I hope the address demonstrates the process of identifying a mathematical problem from a real-world problem, also referred to as the mathematical modelling process, the mathematical analysis involved, and the predictive as well as control aspects of the mathematical models. Above all, good mathematics must be employed to deeply understand the underlying physical behaviour of the problem. Hence the address title.

The study of networks originated from Euler's celebrated paper of 1736 [1] in which the solution to the problem of the seven bridges of Königsbridge is presented. This was the first true proof of the theory of networks. From this event fields of mathematics such as topology, graph theory and discrete mathematics have evolved. In the modern era there are different types of networks, which sometimes are classified as: social networks, information networks (knowledge networks), technological networks, biological networks [2]. Recently, there has been a lot of mathematical research with the emphasis on considering small graphs and the mathematical properties of individual nodes or links within such graphs [3]. A special case of such networks are fluid flow networks.

In general, a network is a set of objects, which are referred to as vertices or sometimes nodes, with connections between them, called edges (see Figure 1). Systems taking the form of networks (also referred to as graphs in much of the mathematical literature) are numerous in the world.

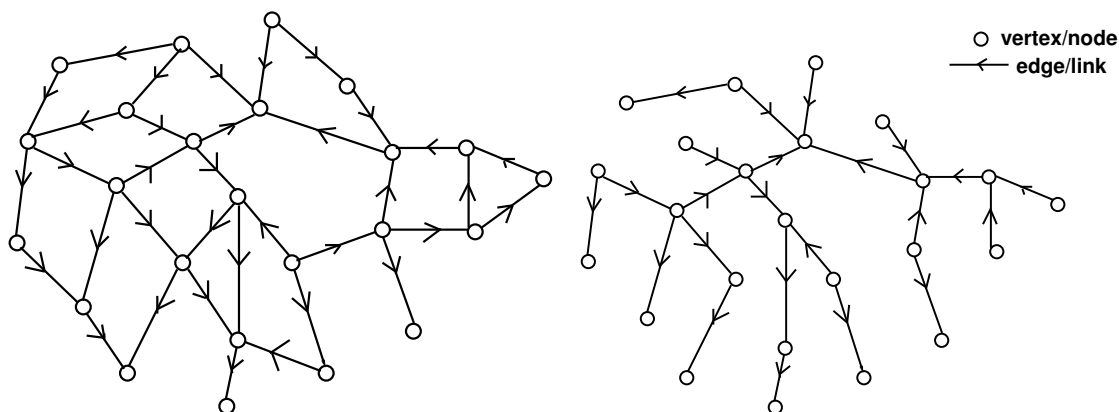


Figure 1: Sketches of two directed networks. The arrows denote the direction of flow.

The graphs or networks we are interested in also evolve over time, with values defined on vertices

and edges changing. The study of networks is by no means a complete science yet [3], and many of the possibilities have yet to be explored in depth. Ours is just a small contribution to the whole discussion and there is still a lot to be done. The ultimate goal of our research is to understand and explain the workings of systems built upon networks, i.e. to look at the behaviour of models of physical (or biological or social) processes taking place in the networks. It is widely acknowledged that progress on this front has been slower than progress on understanding network structure [3].

Of interest in the gas pipeline engineering community is optimisation of the pipeline functions under transient conditions. Thus one has to work with transient flow in natural gas transportation systems. For example, some of the important issues that mathematical modelling or simulation technology can address include optimising pipeline operations to economise costs, and calibrating the performance of a pipeline system. Computerised simulation of pipeline systems in which steady state conditions of distribution networks were considered began in the 1950's. To date transient analysis and inclusion of elements such as valves, compressors and storage fields have been developed. The development of digital codes to undertake the analysis began in the 1970's. Our contribution has been to undertake mathematical analysis, proving well-posedness, of the nodes of flow networks for gas dynamics, optimal control of compressor stations, which are also considered special nodes, as well as the stabilisation of flow on networks through boundary stabilisation.

## 2 Gas flow

In network flow problems, the mathematical model of the underlying physical process is formulated by an interconnected hierarchy of dynamics on the arcs/edges using mathematical modelling principles. These dynamics are coupled and interact with other processes by transmission conditions at the vertices/nodes of the graph. The transmission conditions might obey other independent dynamic laws defined based on physical, chemical or engineering considerations.

Arising mathematical issues deal with modelling and the interaction of different dynamics on arcs and the influence of the transmission conditions on the local and global dynamics of the network. This in particular involves the interaction between different dynamic and/or discrete models. Other problems arise due to the underlying complex physics and governing principles inside the vertices which are usually not known exactly, but need to be formulated in a concise mathematical formulation for further treatment.

From a practical point of view, network problems are usually large-scale and contain additional complexity due to their geometry. Hence, efficient numerical methods and new techniques are required to compute solutions for given accuracy and within a reasonable time. In most cases real-time solutions would be the desired goal.

To address such problems, one considers modelling of the dynamics on the arcs and development or application of efficient and accurate numerical methods for resolving these dynamics. Already developed models are available and can be applied. Where necessary a careful derivation of simplified dynamics which yields a trade-off between accuracy and computability can be considered. The second step is the modelling of transmission or coupling conditions informed by the underlying physical processes and mathematical analysis of the derived conditions. In particular, the compatibility of the coupling with both mathematical and engineering needs are of interest. For example, in the case of gas dynamics in pipelines, results are already available. The details of mathematical proofs of existence of solutions to a coupled system of dynamics on arcs and vertices are presented in [4]. Optimisation techniques for solving optimisation problems based on the space mapping idea are presented in [5]. Further to that, numerical analysis of stabilisation problems can be found in [6].

### 2.1 Flow in a single pipe

To present flow in a network of pipes, it is necessary to consider flow in a single pipe. Thereafter extensions of single pipe flow to coupled pipes in a network will be discussed. The link between the two are algebraic relations which are defined using physical considerations.

The most detailed model, also referred to as the *fine model*, is a non-linear partial differential equation (PDE) which is a simplification of the Euler equations for gas dynamics. Some simplifications assumed on the Euler equations are as follows. For pipelines the cross-section of the pipes is very small compared to the length of the pipeline segments (pipes). Such being the case, the flow is assumed to be

one-dimensional. Hence, pressure and velocity variations across the cross-sectional area are assumed negligible. The temperature of the gas is assumed to be constant. This is the case since most of the pipes in the real-world are buried underground and the soil is assumed to be a large heat sink. Therefore, the flow is assumed to be in thermodynamic equilibrium. Only two forces acting on the gas are considered significant: internal friction of the pipe and inclination of the pipe due to topography.

With these assumptions the isothermal Euler equations in one space dimension augmented with non-linear source terms are obtained [4, 7]:

$$\frac{\partial \rho}{\partial t} + \frac{\partial q}{\partial x} = 0; \quad (1a)$$

$$\frac{\partial(\rho u)}{\partial t} + \frac{\partial}{\partial x} \left( \frac{q^2}{\rho} + p(\rho) \right) = s_1(\rho, u) + s_2(x, \rho). \quad (1b)$$

The first equation defines the conservation of mass. The second equation is based on Newton's laws of motion and describes the conservation of momentum (mass flux of the gas)  $q = \rho u$  where  $\rho(x, t)$  is the mass density of the gas,  $u(x, t)$  is the gas velocity and  $p(\rho)$  is a pressure law. The pressure law satisfies the following properties:

**(P)**  $p \in C^2(\mathbb{R}^+; \mathbb{R}^+)$  with  $p(0) = 0$  and  $p'(\rho) > 0$  and  $p'' \geq 0$  for all  $\rho \in \mathbb{R}^+$ .

With the above assumptions,  $p(\rho)$  is often chosen as

$$p(\rho) = \frac{Z\mathcal{R}T}{M_g} \rho = a^2 \rho, \quad (2)$$

where  $Z$  is the natural gas compressibility factor,  $\mathcal{R}$  the universal gas constant,  $T$  the absolute gas temperature, and  $M_g$  the gas molecular weight. Since temperature has been assumed constant, one considers the constant  $a$  to be the speed of sound in the gas. Also note that  $a$  depends on the type of gas as well as the temperature.

For the sake of simplicity but without losing too many properties of real-world gas flow [8, 9, 10], further assumptions are made: pipe wall expansion or contraction under pressure loads is negligible; hence, pipes have constant cross-sectional area. The diameter,  $D$ , of the pipe is constant.

The source term modelling the influence of friction is modelled by assuming steady state friction for all pipes [8, 11]. The friction factor  $f_g$  is calculated using Chen's equation [12]:

$$\frac{1}{\sqrt{f_g}} := -2 \log \left( \frac{\varepsilon/D}{3.7065} - \frac{5.0452}{N_{Re}} \log \left( \frac{1}{2.8257} \left( \frac{\varepsilon}{D} \right)^{1.1098} + \frac{5.8506}{0.8981 N_{Re}} \right) \right) \quad (3)$$

where  $N_{Re}$  is the Reynolds number  $N_{Re} = \rho u D / \mu$ ,  $\mu$  the gas dynamic viscosity and  $\varepsilon$  the pipeline roughness, which are again assumed to be the same for all pipes. With the above assumptions, the friction term takes the form

$$s_1(\rho, u) = -\frac{f_g}{2D} \rho u |u|.$$

The pipe inclination takes the form

$$s_2(x, \rho) = -g \rho \sin \alpha(x)$$

where  $g$  is acceleration due to gravity and  $\alpha(x)$  is the slope of the pipe.

In addition, two additional assumptions need to be made:

**A1.** There are no vacuum states, i.e.  $\rho > 0$ .

**A2.** All flow states are subsonic, i.e.  $\frac{q}{\rho} < a$ .

These assumptions are backed by physical considerations. It is reasonable to assume that atmospheric pressure is the lower bound for the pressure in the pipes. Lower pressure can occur due to waves travelling through the pipe. Waves which would create vacuum states are untenable since they would cause the pipe to explode or implode. Generally pipelines are operated at high pressure (40 to 60 bar) and the gas velocity is very low ( $< 10$  m/s). As the speed of sound in natural gas is around 370 m/s, the second

assumption also makes sense. In pipeline networks, all states are a reasonable distance from the sonic states so that travelling waves cannot create sonic or supersonic states.

Briefly, some mathematical properties of the above system will be discussed [13]. These mathematical properties are used to discuss the well-posedness of the flow problem in a single pipe. With the above assumptions Equation (1) are also strictly hyperbolic. If an initial condition is given, the problems are also referred to as Cauchy problems. These admit discontinuous solutions or shock solutions and need to be treated in a weak topology. For mathematical analysis it is common practice to consider Equation (1) with discontinuous initial solutions, the so-called Riemann problem. To solve Riemann problems, characteristic fields based on Lax-curves are employed [14, 13].

## 2.2 Flow in networks or coupling pipes and nodes

To complete the discussion of flows in networks it is necessary to discuss coupling of different pipes at a node. Coupling of pipes is believed to be the major part of gas networks [10]. Approaches in the engineering community are exploited.

Applying assumption **A2** and the notation in [15, 4], a network of pipes is defined as a finite directed graph  $(\mathcal{J}, \mathcal{V})$  where  $\mathcal{J}$  is a set of edges and  $\mathcal{V}$  is a set of nodes. Both sets are taken to be non-empty. Each edge  $j \in \mathcal{J}$  corresponds to a pipe parametrised by an interval  $\mathcal{I}_j := [x_j^a, x_j^b]$ . Each node  $v \in \mathcal{V}$  corresponds to a single intersection of pipes. For each node  $v \in \mathcal{V}$ , the set of all indices of pipes  $j \in \mathcal{J}$  ingoing and outgoing to the node can be separated into two sets  $\delta_v^-$  and  $\delta_v^+$ , respectively. The set of all pipes intersecting at a node  $v \in \mathcal{V}$  can be denoted as  $\delta_v = \delta_v^- \cup \delta_v^+$ . In addition, the degree of a vertex  $v \in \mathcal{V}$  is the number of pipes connected to the node.

Further, the nodes  $\mathcal{V}$  can also be classified according to their physical utility. Any node of degree one, i.e.  $|\delta_v^- \cup \delta_v^+| = 1$ , is either an inflow ( $\delta_v^- = \emptyset$ ) or an outflow ( $\delta_v^+ = \emptyset$ ) boundary node for the network. These nodes can be interpreted as suppliers or consumers of gas and the sets of such nodes can be denoted as  $\mathcal{V}_I$  or  $\mathcal{V}_O$ , respectively. Some nodes of degree two are controllable nodes (for example, compressor stations or valves). This subset of nodes is denoted by  $\mathcal{V}_C \subset \mathcal{V}$ . The rest of the nodes,  $\mathcal{V}_P = \mathcal{V} \setminus (\mathcal{V}_I \cup \mathcal{V}_O \cup \mathcal{V}_C)$ , can be considered the standard pipe-to-pipe intersections.

In addition to the above assumptions, the following can also be imposed:

**A3.** All pipes have the same diameter  $D$ . The cross-sectional area is given by  $A = \frac{D^2}{4}\pi$ . Similar to a single pipe, the walls do not expand or contract due to pressure load.

**A4.** The friction factor,  $f_g$ , is the same for all pipes.

In general, the value at a node  $v$  depends only on the flow in the ingoing and outgoing pipes and where needed some (possibly) time-dependent controls. Thus for the network, on each edge  $l \in \mathcal{J}$ , assume that the dynamics is governed by the isothermal Euler equations (1) for all  $x \in [x_l^a, x_l^b]$  and  $t \in [0, T]$  supplemented with initial data  $U_l^0$ . In addition, on each vertex  $v \in \mathcal{V}$  systems of the type (1) are coupled by suitable coupling conditions:

$$\Psi(\rho^{(l_1)}, q^{(l_1)}, \dots, \rho^{(l_n)}, q^{(l_n)}) = \Pi(t), \quad \delta_v = \{l_1, \dots, l_n\}.$$

Hence the network model for gas flow in pipelines consisting of  $m$  pipes takes the form

$$\frac{\partial \rho^{(l)}}{\partial t} + \frac{\partial q^{(l)}}{\partial x} = 0; \tag{4a}$$

$$\frac{\partial q^{(l)}}{\partial t} + \frac{\partial}{\partial x} \left( \frac{(q^{(l)})^2}{\rho} + a^2 \rho^{(l)} \right) = s(x, \rho^{(l)}, q^{(l)}), \quad l \in \{1, \dots, m\}; \tag{4b}$$

$$\Psi(\rho^{(l_1)}, q^{(l_1)}, \dots, \rho^{(l_n)}, q^{(l_n)}) = \Pi(t). \tag{4c}$$

Now let us consider different junctions and the resulting coupling conditions.

### 2.2.1 Inflow and outflow nodes

The inflow and outflow nodes  $v \in \mathcal{V}_I \cup \mathcal{V}_O$  can be identified with boundary conditions for the Equations (1), modelling time-dependent inflow pressure or the outgoing mass flux of the gas. This formulation is well known and widely discussed in the literature [13].



### 2.2.2 Standard junctions

On junctions  $v \in \mathcal{V}_P$ , the amount of gas is conserved at pipe-to-pipe intersections:

$$\sum_{l \in \delta_v^+} q^{(l)} = \sum_{\bar{l} \in \delta_v^-} q^{(\bar{l})}$$

In addition, pressure is assumed equal for all pipes at the node [16, 17, 9], i.e.

$$p(\rho^{(l)}) = p(\rho^{(\bar{l})}), \quad \forall l, \bar{l} \in \delta_v^- \cup \delta_v^+.$$

An introduction of such coupling conditions was undertaken in [7] and analysed in [4]. The conservation of mass at the nodes is unanimously agreed upon in the literature. The pressure conditions, however provide room for debate. The engineering community apply pressure tables but it is still not clear how these can be represented in mathematical terms. Different conditions can be applied [18]. Here we assume there is ‘good mixing’ at each vertex so that the condition of equal pressure can be imposed. Hence at the vertex the pipes are coupled using the following conditions:

$$\Psi(\rho^{(l_1)}, q^{(l_1)}, \dots, \rho^{(l_n)}, q^{(l_n)}) = \begin{pmatrix} \sum_{l \in \delta_v^+} q^{(l)} - \sum_{\bar{l} \in \delta_v^-} q^{(\bar{l})} \\ p(\rho^{(l_1)}) - p(\rho^{(l_2)}) \\ \dots \\ p(\rho^{(l_1)}) - p(\rho^{(l_n)}) \end{pmatrix} = 0 \quad (5)$$

for  $\delta_v^- \cup \delta_v^+ = \{l_1, \dots, l_n\}$ .

To solve the problem at the vertex, ideas from solutions of the standard Riemann problem are adopted [13, 14, 19]. Half-Riemann problems are solved instead [20]. It is believed this was one of the most important breakthroughs in the mathematical analysis of networked flow nodes. In addition to that a few remarks on the process are in order. Given a node with  $n$  pipes coupled through coupling conditions (5), in each of the  $n$  pipes assume a constant subsonic state  $(\bar{\rho}^{(l)}, \bar{q}^{(l)})$ . The states  $(\bar{\rho}^{(1)}, \bar{q}^{(1)}), \dots, (\bar{\rho}^{(n)}, \bar{q}^{(n)})$  need not satisfy the coupling conditions. Hence, similar to the Riemann problem, the Lax curves can be used to construct the intermediate states that develop at the node. Unfortunately, solutions to this problem are only realisable if the waves generated travel with negative speed in incoming pipes and with positive speed in outgoing pipes, which means the coupling conditions do not provide feasible solutions to all choices of states  $(\bar{\rho}^{(1)}, \bar{q}^{(1)}), \dots, (\bar{\rho}^{(n)}, \bar{q}^{(n)})$ .

The coupling conditions as presented above are well-posed. This result was discussed in [4, 20]. This is arguably our most important contribution to the mathematical analysis of gas flow at the node. Below a numerical example will be presented. In addition, this work has been extended further to prove well-posedness for multi-phase flows. The special case of the drift-flux model has been investigated in [21].

At this point an example taken from [4] is presented. Consider an incoming wave on pipe  $l = 1$ , which cannot freely pass the intersection, due to a given low flux profile on the outgoing pipe  $l = 2$ . Friction in the pipes is taken to be  $f_g = 10^{-3}$ . The sound speeds are  $a_l = 360$  m/s and the pipe diameter is  $D = 0.1$  m. An inflow of  $q_{in} = 70$  kg m<sup>-2</sup>s<sup>-1</sup> at  $x = x_1^a$  and an outflow of  $q_{out} = 1$  at  $x = x_2^b$  is prescribed. Both pipes have the same initial condition  $U_j^0 = [\frac{1}{360}, 1]$ . In Figure 2, snapshots of the density evolution are shown. Take note that the inflow profile moves on pipe 1 until it reaches the intersection. Since the maximal flow on the outgoing pipe is  $q^* = 1$ , a backwards moving shock wave on pipe 1 develops and increases the density near the intersection.

### 2.2.3 Controllable nodes

At controllable nodes one may think about objects that are used to regulate the flow. What comes to mind are valves and compressor stations. The compressor will be discussed here since it is used to regulate the flow at a prescribed level in order to satisfy the needs of consumers. The compressor acts as a directed external force, which means gas is only pumped in one direction. In this case the degree of the junction is two.

Denote the ingoing quantities by  $v-$  and the outgoing ones by  $v+$ . Assuming the compressors are

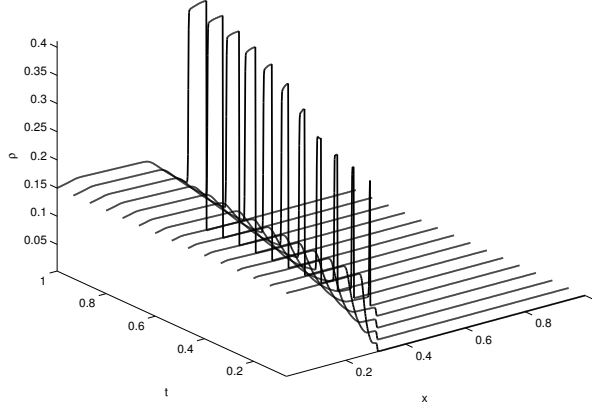


Figure 2: Snapshots of the solution  $\rho_l$  to the problem of two connected pipes at different times  $t$  [4].

powered by external energy, then the amount of gas is conserved at controllable nodes [20]

$$q^{(v-)} = q^{(v+)}.$$

The effect of the compressor can be modelled as a second coupling condition of the form [22]

$$P_v(t) = q^{(v-)} \left( \left( \frac{p(\rho^{(v+)})}{p(\rho^{(v-)})} \right)^\kappa - 1 \right) \quad (6)$$

where  $\kappa$  is a parameter of the gas defined by  $\kappa = \frac{\gamma - 1}{\gamma}$  using the isentropic coefficients  $\gamma \in \left\{ \frac{5}{3}, \frac{7}{5} \right\}$  of the gas. Note that the time-dependent power of the compressor is proportional to  $P_v(t)$ . Further,  $q^{(v-)} > 0$  by assumption. Hence, the coupling for  $q^{(v-)} \leq 0$  is given by the standard node conditions.

For the compressor station the coupling conditions are given by

$$\Psi(\rho^{(v-)}, q^{(v-)}, \rho^{(v+)}, q^{(v+)}) = \begin{pmatrix} q^{(v-)} - q^{(v+)} \\ q^{(v-)} \left( \left( \frac{p(\rho^{(v+)})}{p(\rho^{(v-)})} \right)^\kappa - 1 \right) \end{pmatrix} = \begin{pmatrix} 0 \\ P_v(t) \end{pmatrix}. \quad (7)$$

It is interesting to note that if the compressor is turned off, ( $P_v = 0$ ), the second coupling condition in (7) reduces to  $p(\rho^{(v+)}) = p(\rho^{(v-)})$ . It is therefore clear that the coupling conditions of the compressor are indeed a generalisation of the coupling conditions at standard junctions of degree two.

The Lax curves can also be used to illustrate how the compressor works [20]. In summary, one can show that mathematically the compressor increases the pressure in the outgoing pipe at the expense of the pressure in the incoming pipe. Furthermore, the pressure in the outgoing pipe cannot be increased arbitrarily, since the maximum flux at the junction is bounded. This is consistent with the expected behaviour of a compressor.

### 3 Optimal control

Compressors are one of the most costly devices to operate. Energy suppliers, therefore, are interested in understanding how to optimally control the compressors in order to deliver gas to consumers at pre-determined contract conditions. An attempt to develop an optimal control procedure was made using the idea of space mapping. For this, one needs a cheap (efficient) model to drive the optimal control process and an expensive model (*fine model*) to correct the solution of the cheap model.

The *fine model* based on isothermal Euler equations, Equation (1), is considered here. For this model, let us assume that  $s_2 = 0$ , i.e. ignoring the pipe inclination. Further, the model of the compressor station is the one given in Equation (6).

Assuming that  $u \ll 1$  then the fine model simplifies to:

$$\frac{\partial \rho}{\partial t} + \frac{\partial q}{\partial x} = 0 \quad (8a)$$

$$\frac{\partial q}{\partial t} + \frac{\partial p(\rho)}{\partial x} = -f_g \frac{q|q|}{\rho} = s_1(\rho, q). \quad (8b)$$

The assumption of small velocities in gas networks has been made in high-pressure gas networks. In such cases, changes in the demand and supply only occur on a time-scale of hours. Typically values for velocities and pressure are  $u = 10 \frac{\text{m}}{\text{s}}, p = 70 \text{ bar}, t = 1 \text{ h}$  and the length of the pipe is  $10^5 \text{ m}$ . Therefore,  $\frac{\partial \rho u^2}{\partial x} = 0.05 \frac{\text{N}}{\text{m}^3}$  which is small compared to the pressure gradient of  $\frac{\partial p}{\partial x} = 70 \frac{\text{N}}{\text{m}^3}$ .

A further simplification is to consider a steady state version of (8), i.e.  $\frac{\partial \rho}{\partial t} = 0$  and  $\frac{\partial q}{\partial t} = 0$ , to obtain one of the most basic models also referred to as *the algebraic model*. This makes sense if the dynamics at the boundary are much slower than the flow and pressure dynamics in the pipe. One only accounts for the pressure drop due to pipe-wall friction. Hence, for a single pipe the model reduces to

$$\frac{\partial q}{\partial x} = 0, \quad (9a)$$

$$\frac{\partial p(\rho)}{\partial x} = s_1(\rho, q). \quad (9b)$$

Integrating the model analytically yields a stationary mass flux in the pipe and a square-root shaped density profile along the pipe. To close the system one needs to define boundary conditions induced by coupling conditions at compressor stations presented in Equation (7). It is worth noting that due to the inlets to and outlets of the network the functions  $q$  and  $\rho$  are in general time-dependent. In summary, the *coarse model* consists of the equations (9), (7) and initial conditions.

It can be remarked here that in terms of computational cost there is a significant difference between the *fine* and *coarse* models. The PDEs (1) are solved by second-order finite-volume schemes with  $N_{\Delta t}$  and  $N_{\Delta x}$  discretization points in time and space, respectively. Since explicit schemes are applied, the discretization points  $N_{\Delta t}$  and  $N_{\Delta x}$  are chosen so that the CFL-condition is satisfied. It should be expected that the solution to the non-linear PDE is computationally far more expensive than the solution to the algebraic model.

To solve the optimal control problem efficiently one needs to apply the *coarse* model. However, the *fine* model defines more dynamics and its optimisation is the desired objective. To achieve the desired pressure levels compressor stations must be run to compensate for pressure losses due to internal pipe friction. This is the major industrial problem. Mathematically, this problem is formulated as an optimisation problem for the unknown compressor.

The inflow pressure  $p(x_1^a, t)$  and the outflow mass flux  $q(x_2^b, t)$  of this simple network are given. One needs to approximate a certain desired outlet pressure  $\bar{p}(t) = p(\bar{\rho}(t))$  at  $x = x_2^b$  within a requisite time-horizon of  $T$  by adjusting the compressor power  $P_v(t)$ . The power is therefore *the control variable*. The solution,  $P_v^*(t)$ , is therefore obtained by solving the following optimisation problem

$$P_v^*(t) = \arg \min_{P_v(t) \in \mathcal{P}_{\text{adm}}} \frac{1}{2} \int_0^T (p(x_2^b, t) - \bar{p}(t))^2 dt \text{ subject to (4) for } l = 1, 2, \text{ and (7);} \quad (10a)$$

$$p_{\text{in}}(t), \quad q_{\text{out}}(t) \quad t \in (0, T) \quad (10b)$$

where  $p_{\text{in}}$  is pressure at inlet to the network,  $q_{\text{out}}$  is the given outlet mass flux and  $\mathcal{P}_{\text{adm}}$  is a set of all *admissible controls*  $P_v$ .

Apart from efficiency issues, the second more technical reason to consider the algebraic model is that the non-linear model admits discontinuous solutions which complicate the calculus needed to solve optimisation problems [23, 24, 25]. Hence the approach developed here is to only involve simulations of (4). The approach uses space mapping [26, 27] to estimate the derivatives of the objective function. The non-linear model is only used to verify the estimates.

Within the context of the gas network the outlet pressure for the compressor power  $P_v(t)$  based on

the *fine scale model* is therefore

$$\mathcal{F}(P_v)(t) := p(x_2^b, t).$$

Similarly, for given inlet pressure and outlet mass flux data, the algebraic model (9) and (7), the *coarse scale model*, are solved. The control is the same as for the fine model. The coarse model response is easier to evaluate and is denoted by

$$\mathcal{C}(P_v)(t) := p(x_2^b, t).$$

The real benefit of applying the coarse model lies in the shorter computational time.

Using the previously defined functionals, problem (10) is equivalent to

$$\min \frac{1}{2} \int_0^T \left( \mathcal{F}(P_v)(t) - \bar{p}(t) \right)^2 dt \text{ subject to (1) for } l = 1, 2, \text{ and (7)}. \quad (11)$$

The minimizer to (11) is denoted by  $P_{v\mathcal{F}}^*$ . Hence an alternative problem is posed: For a given function  $\bar{p}(t)$ , solve

$$\min \frac{1}{2} \int_0^T \left( \mathcal{C}(P_v)(t) - \bar{p}(t) \right)^2 dt \text{ subject to (9) for } l = 1, 2, \text{ and (7)}. \quad (12)$$

The solution to problem (12) is denoted by  $P_{v\mathcal{C}}^*(t; \bar{p})$ . The existence of  $P_{v\mathcal{C}}^*(t; \bar{p})$  is necessary in order to obtain a well-defined space mapping algorithm.

The space mapping functional  $P_v \rightarrow \mathcal{Q}(P_v)$  can be defined as

$$\mathcal{Q}(P_v) = \arg \min_{P_{v\mathcal{C}}(t)} \frac{1}{2} \int_0^T \left( \mathcal{C}(P_{v\mathcal{C}})(t) - \mathcal{F}(P_v)(t) \right)^2 dt. \quad (13)$$

*Perfect matching* is defined as the case in which

$$P_{v\mathcal{C}}^*(t; \bar{p}) = \mathcal{Q}(P_{v\mathcal{F}}^*)(t) = \arg \min_{P_{v\mathcal{C}}(t)} \frac{1}{2} \int_0^T \left( \mathcal{C}(P_{v\mathcal{C}})(t) - \mathcal{F}(P_{v\mathcal{F}}^*)(t) \right)^2 dt. \quad (14)$$

The desired aim is to find

$$\mathcal{Q}(P_{v\mathcal{F}}^*)(t) \approx P_{v\mathcal{C}}^*(t; \bar{p})$$

for the desired data  $\bar{p}$ .

Following the stated algorithm, it is required to determine  $P_{v\mathcal{C}}^*$ , possibly an approximation

$$\mathcal{Q}(P_v^*)(t) = P_{v\mathcal{C}}^*(t; \bar{p}). \quad (15)$$

The solution,  $P_v^*$ , of Equation (15) is then denoted  $P_{v\mathcal{F}}^*$ .

#### Existence of solutions to (12):

For a simple geometry of two connected pipes the algebraic model can be integrated exactly. Furthermore, the solution  $t \rightarrow P_{v\mathcal{C}}^*(t; \bar{p})$  to (12) exists provided that the desired pressure profile satisfies

$$\bar{p}^2(t) \geq \rho_{\text{in}}^2(t) - \frac{2(x_2^b - x_1^a)f_g}{a^2} |q_{\text{out}}(t)| q_{\text{out}}(t) > 0 \quad (16)$$

and  $q_{\text{out}}(t) \geq 0$ .

#### Existence of solutions to (11):

Assume that a solution  $P_v^*$  for (15) is obtained for  $P_{v\mathcal{C}}^*(t; \bar{p})$ , then since  $\mathcal{Q}$  is in this case a perfect mapping, it can be deduced that

$$\mathcal{F}(P_v^*)(t) = p(\rho_{\text{in}}(t)). \quad (17)$$

This also implies that  $P_v^*$  is a solution to (11). Hence the following proposition:

**Proposition 3.1.** *Assume a network consists of two pipes connected by a single compressor. Assume inlet pressure data is  $p_{\text{in}}(t)$  and outlet mass flux data is  $q_{\text{out}}(t) \geq 0$  and a desired pressure*

profile  $\bar{p}$  be given such that (16) is satisfied.

A solution to (15) exists if and only if a solution to (11) exists.

It needs to be noted here that there is a major difference in the behavior of solutions to (4) and (9): the hyperbolic equation generates waves traveling with *finite* speed of propagation while in the algebraic model perturbations travel instantaneously (infinite speed). This means that the coarse model needs to estimate the speed of propagation.

Now an example is presented. The speed of sound for the gas under consideration is 380 [m/s] and constant initial density of  $\bar{\rho} = 105$  [kg/m<sup>3</sup>] at the inlet of the first pipe and a non-stationary mass flux  $\bar{q}(t) = 80 + \sin(\frac{1}{10}\pi t)$  at the outlet of the second pipe is prescribed [5]. The desired density is an s-shaped profile connecting the densities  $\rho = 100$  and  $\rho = 105$  and then linearly decreasing until  $\rho = 102$  within a given time horizon of  $T = 36$ . Figure 3 shows that the final outlet pressure evolutions show the same qualitative and quantitative behavior. Therefore, the presented optimisation approach is mesh-independent. Further, sufficiently good agreement between the desired and the obtained pressure evolution is obtained for  $N_{\Delta P} \geq 40$ ; c.f. the clipping in the right part of the figure.

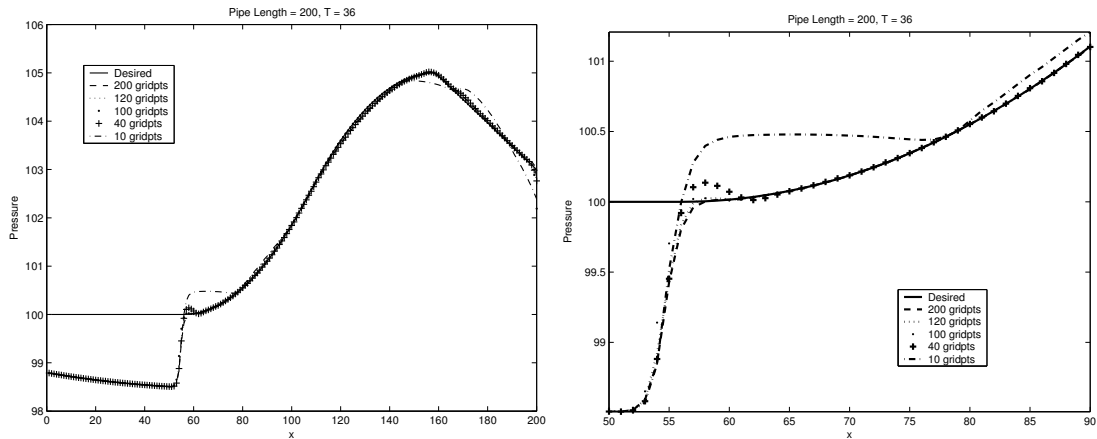


Figure 3: Pressure evolution for optimized compressor control. The compressor control is discretized using  $N_{\Delta P} \in \{10, \dots, 200\}$  discretization points. The evolution for  $t \in [50, 90]$  is shown in more detail in the right part of the figure [5].

## 4 Boundary stabilisation

The significant tool that has been introduced in the study of boundary stabilisation problems are suitable Lyapunov functions. For stability of the solution to the partial differential equation, the exponential decay of such a Lyapunov function can be established in a variety of cases – see [28] for example. For a more detailed discussion, the reader may refer to [30] and the references therein. Our focus was the analysis of the numerical discretisation analogous to the continuous results. Therefore, the conditions under which in a numerical scheme an exponential decay of the discrete solution to the hyperbolic system can be observed were derived [6]. Mathematical proofs for explicit decay rates for general three-point finite volume schemes, using the discrete counterpart of the Lyapunov function, are presented in [6]. In general, the exponential decay of discrete  $L^2$ -Lyapunov functions up to a given finite terminal time only has been proved.

### 4.1 The continuous results

The following results are (probably) the most generally available continuous stabilisation results [28, 29]. Consider the non-linear hyperbolic partial differential equation

$$\frac{\partial u}{\partial t} + \frac{\partial f(u)}{\partial x} = 0, \quad u(x, 0) = u^0(x), \quad (18)$$

where  $t \in [0, +\infty)$ ,  $x \in [0, L]$ ,  $u : [0, +\infty) \times [0, L] \rightarrow \mathbb{R}^p$  and  $f : \mathbb{R}^p \rightarrow \mathbb{R}^p$  denotes a possibly non-linear smooth flux function. The gas dynamics model discussed above is a special case of this with  $p = 2$ . The flux function  $f$  is assumed to be strictly hyperbolic. If the solution,  $u$ , is smooth, solving Equation (18) is equivalent to solving

$$\frac{\partial u}{\partial t} + F(u) \frac{\partial u}{\partial x} = 0, \quad x \in [0, L], t \in [0, +\infty), u \in \mathbb{R}^p \quad (19)$$

with  $F(u) = D_u f(u)$  a  $p \times p$  real matrix and

$$u(x, 0) = u^0(x). \quad (20)$$

Consider the case where  $L = 1$  and hence  $x \in [0, 1]$ . In addition,  $\|a\|_q$  denotes the  $q$ -norm of the vector  $a \in \mathbb{R}^p$ ,  $p > 1$ , and  $\|x\|$  denotes the absolute value of a real number  $x \in \mathbb{R}$ .

Feedback boundary conditions [28, 30, 31] for (19) can be prescribed as follows:

$$\begin{pmatrix} u_+(t, 0) \\ u_-(t, 1) \end{pmatrix} = G \begin{pmatrix} u_+(t, 1) \\ u_-(t, 0) \end{pmatrix}, \quad t \in [0, +\infty) \quad (21)$$

where  $G : \mathbb{R}^p \rightarrow \mathbb{R}^p$  is a possible non-linear function. The variables  $u_+$  and  $u_-$  will be defined at a later stage below. Denote by  $\Lambda_i$  for  $i = 1, \dots, p$  the eigenvalues of  $F(0)$ . As in [28],  $F(0)$  may be assumed to be diagonal (otherwise an appropriate state transformation is applied). Due to the strict hyperbolicity the eigenvalues are distinct, i.e.  $\Lambda_i \neq \Lambda_j$  for  $i \neq j$ . In addition, assume that  $\Lambda_i \neq 0$  for all  $i = 1, \dots, p$ . The eigenvalues are ordered such that  $\Lambda_i > 0$  for  $i = 1, \dots, m$  and  $\Lambda_i < 0$  for  $i = m + 1, \dots, p$ . For any  $u \in \mathbb{R}^p$ , define  $u_+ \in \mathbb{R}^m$  and  $u_- \in \mathbb{R}^{p-m}$  by requiring

$$u = \begin{pmatrix} u_+ \\ u_- \end{pmatrix}.$$

Hence,  $u_{\pm}$  are the components of the vector  $u \in \mathbb{R}^p$  corresponding to the positive and negative eigenvalues of the diagonal matrix  $F(0)$ . Similarly, for  $F$  (and  $G$ ), define for  $F_+ : \mathbb{R}^p \rightarrow \mathbb{R}^{m \times p}$ ,  $G_+ : \mathbb{R}^p \rightarrow \mathbb{R}^m$  and  $F_- : \mathbb{R}^p \rightarrow \mathbb{R}^{(p-m) \times p}$ ,  $G_- : \mathbb{R}^p \rightarrow \mathbb{R}^{p-m}$  by

$$F(u) = \begin{pmatrix} F_+(u) \\ F_-(u) \end{pmatrix} \quad \text{and} \quad G(u) = \begin{pmatrix} G_+(u) \\ G_-(u) \end{pmatrix}.$$

Again, assume that  $F_{\pm}(u)$  and  $G_{\pm}(u)$  are diagonal, for all  $u$ . Let  $G_+(u) = G_+((u_+, u_-)^T)$ . The partial derivatives with respect to  $u_+$  and  $u_-$  will be denoted by  $G'_{+,u_+}(u)$  and  $G'_{+,u_-}(u)$ , respectively and analogously for  $G_-$ . This notation is as in [28]. Then, the definition of stability of the equilibrium solution  $u \equiv 0$  is given by:

**Definition 4.1** (Definition 2.2[28]). *The equilibrium solution  $u \equiv 0$  of the non-linear system (19)-(20) is exponentially stable (in the  $H^2$ -norm) if there exists  $\epsilon > 0$ ,  $\nu > 0$ ,  $C > 0$  such that, for every  $u^0 \in H^2((0, 1); \mathbb{R}^p)$  satisfying  $\|u^0\|_{H^2((0,1); \mathbb{R}^p)} \leq \epsilon$  and the compatibility conditions*

$$\begin{aligned} \begin{pmatrix} u_+^0(0) \\ u_-^0(1) \end{pmatrix} &= G \begin{pmatrix} u_+^0(1) \\ u_-^0(0) \end{pmatrix}; \\ F_+(u^0(0))u_x^0(0) &= G'_{+,u_+} \begin{pmatrix} u_+^0(1) \\ u_-^0(0) \end{pmatrix} F_+(u^0(1))u_x^0(1) + G'_{+,u_-} \begin{pmatrix} u_+^0(1) \\ u_-^0(0) \end{pmatrix} F_-(u^0(0))u_x^0(0); \\ F_-(u^0(1))u_x^0(1) &= G'_{-,u_+} \begin{pmatrix} u_+^0(1) \\ u_-^0(0) \end{pmatrix} F_+(u^0(1))u_x^0(1) + G'_{-,u_-} \begin{pmatrix} u_+^0(1) \\ u_-^0(0) \end{pmatrix} F_-(u^0(0))u_x^0(0); \end{aligned}$$

the classical solution  $u$  to the Cauchy problem (19) and (20) with boundary conditions (21) is defined for all  $t \in [0, +\infty)$  and satisfies

$$\|u(\cdot, t)\|_{H^2((0,1); \mathbb{R}^p)} \leq C \exp(-\nu t) \|u^0\|_{H^2((0,1); \mathbb{R}^p)}. \quad (22)$$

For any real  $p \times p$  matrix  $A$ ,  $\rho_1(A) := \inf\{\|\Delta A \Delta^{-1}\|_2 : \Delta \in \mathcal{D}_{p,+}\}$ , where  $\mathcal{D}_{p,+}$  is the set of all real

$p \times p$  diagonal matrices with strictly positive diagonal elements. Then, the following general result holds:

**Theorem 4.2** (Theorem 2.3[28]). *Assume  $F(0)$  is diagonal with distinct and non-zero eigenvalues and  $F$  is of class  $C^2(\mathbb{R}^p; \mathbb{R}^p)$  in a neighbourhood of zero. Take  $F(0) = \text{diag}(\Lambda_i)_{i=1}^p$  and  $\Lambda_i > 0$  for  $i = 1, \dots, m$  and  $\Lambda_i < 0$  for  $i = m + 1, \dots, p$  and  $\Lambda_i \neq \Lambda_j$ . Assume  $G$  is of class  $C^2(\mathbb{R}^p; \mathbb{R}^p)$  in a neighbourhood of zero and  $G(0) = 0$ .*

*Let  $\rho_1(G'(0)) < 1$ , then the equilibrium  $u \equiv 0$  for (19) with boundary conditions given by (21) is exponentially stable.*

In this context our contribution was to develop the analysis of the Lyapunov function for a discrete case. Up to now a discrete counter-part to Theorem 4.2 has not been proved. A weaker result concerning the  $L^2$ -stabilisation was developed in [5].

## 4.2 Stabilisation of a discrete problem

The finite volume numerical schemes for boundary  $L^2$ -stabilisation of one-dimensional non-linear hyperbolic systems were adopted. In order to facilitate the proofs, we will need additional assumptions discussed below.

The boundary conditions are considered as in (21) with  $G$  being a diagonal matrix. To simplify the discussion, let

$$F(u) = \text{diag}(\Lambda_i(u))_{i=1}^m, \quad \Lambda_i(u) > 0, \quad \Lambda_i(u) \neq \Lambda_j(u), \quad i \neq j. \quad (23)$$

In the following  $\vec{u}$  denotes all components of  $u$ , i.e.,  $\vec{u} := (u_j)_{j=1}^m$ . Let  $\delta > 0$  and denote by  $M_\delta(0) := \{\vec{u} : |u_j| \leq \delta, j = 1, \dots, m\}$ . Assume  $\delta$  is sufficiently small such that

$$M_\delta(0) \subset B_\epsilon(0).$$

Further, let  $\Delta x$  denote the cell width of a uniform spatial grid and  $N$  the number of cells in the discretisation of the domain  $[0, 1]$  such that  $\Delta x N = 1$  with cell centres at  $x_i = (i + \frac{1}{2})\Delta x$ ,  $i = 0, \dots, N - 1$ . Further  $x_{-1}$  and  $x_N$  denote the cell centres of the cells outside the computational domain on the left-hand and right-hand side of the domain, respectively. The interfacial numerical fluxes are computed at cell boundaries  $x_{i-1/2} = i\Delta x$  for  $i = 0, \dots, N$ . The left and right boundary points are at  $x_{-1/2}$  and  $x_{N-1/2}$ , respectively. The temporal grid is chosen such that the CFL condition holds:

$$\lambda \frac{\Delta t}{\Delta x} \leq 1, \quad \lambda := \max_{j=1, \dots, m} \max_{\vec{u} \in M_\delta(0)} \Lambda_j(\vec{u}) \quad (24)$$

and  $t^n = n\Delta t$  for  $n = 0, 1, \dots, K$  where by possibly further reducing  $\Delta t$ , it can be assumed that  $K\Delta t = T$ . The value of  $u_j(x, t)$  at the cell centre  $x_i$  is approximated by  $u_{i,j}^n$  for  $i = 0, \dots, N - 1$  and for each component  $j$  at time  $t^n$  for  $n = 0, 1, \dots, K$ . The left boundary is discretized using  $u_{-1,j}^n$ . The initial condition is discretized as

$$u_{i,j}^0 := \frac{1}{\Delta x} \int_{x_{i-1/2}}^{x_{i+1/2}} u_j^0(x) dx$$

where  $u_j^0(x)$ ,  $j = 1, \dots, m$  denotes the components of solution vector  $\vec{u}$ .

Hence, the following discretisation of (19)–(21) for  $n = 0, \dots, K - 1$  is introduced:

$$u_{i,j}^{n+1} = u_{i,j}^n - \frac{\Delta t}{\Delta x} \Lambda_j(\vec{u}_i^n) (u_{i,j}^n - u_{i-1,j}^n), \quad i = 0, \dots, N - 1; \quad (25a)$$

$$u_{-1,j}^{n+1} = \kappa_j u_{N-1,j}^{n+1}; \quad (25b)$$

$$u_{i,j}^0 = \frac{1}{\Delta x} \int_{x_{i-1/2}}^{x_{i+1/2}} u_j^0(x) dx, \quad i = 0, \dots, N - 1; \quad j = 1, \dots, m; \quad (25c)$$

$$u_{-1,j}^0 = \kappa_j u_{N-1,j}^0. \quad (25d)$$

Note that the last condition is the discrete compatibility condition for  $u^0$ .

The discrete Lyapunov function at time  $t^n$  with positive coefficients  $\mu_j$ ,  $j = 1, \dots, m$  takes the form

$$L^n = \Delta x \sum_{i=0}^{N-1} \sum_{j=1}^m (u_{i,j}^n)^2 \exp(-\mu_j x_i). \quad (26)$$

The numerical result is as follows:

**Theorem 4.3.** *Let  $T > 0$  and assume (23) holds. For any  $\kappa_j$ ,  $j = 1 \dots, m$  such that*

$$0 < \kappa_j < \sqrt{\frac{D_j^{\min}}{D_j^{\max}}}, \quad (27)$$

where  $\max_{\vec{u} \in M_\delta(0)} \frac{\Delta t}{\Delta x} \Lambda_j(\vec{u}) =: D_j^{\max} \leq 1$  and  $\frac{\Delta t}{\Delta x} \Lambda_j(\vec{u}_i^n) \geq \min_{\vec{u} \in M_\delta(0)} \frac{\Delta t}{\Delta x} \Lambda_j(\vec{u}) =: D_j^{\min} > 0$  the following holds: there exists  $\mu_j > 0$ ,  $j = 1, \dots, m$  and  $\delta > 0$  such that for all initial data  $u_{i,j}^0$  with  $\|u_{i,j}^0\| \leq \delta$ ,  $\|\frac{u_{i,j}^0 - u_{i-1,j}^0}{\Delta x}\| \leq \delta$ , and  $\|\frac{u_{0,j}^n - u_{1,j}^n}{\Delta x}\| \leq \delta \exp\left(t^n \max_{\xi \in M_\delta(0)} \|\nabla_{\vec{u}} \Lambda_j(\vec{\xi})\|_\infty\right)$  for all  $i = 0, \dots, N-1$ ;  $j = 1, \dots, m$ , the numerical solution  $u_{i,j}^n$  defined by (25) satisfies

$$L^n \leq \exp(-\nu t^n) L^0, \quad n = 0, 1, \dots, K \quad (28)$$

for some  $\nu > 0$ . Moreover,  $u_{i,j}^n$  is exponentially stable in the discrete  $L^2$ -norm

$$\Delta x \sum_{i=0}^{N-1} \sum_{j=1}^m (u_{i,j}^n)^2 \leq \tilde{C} \exp(-\nu t^n) \Delta x \sum_{i=0}^{N-1} \sum_{j=1}^m (u_{i,j}^0)^2, \quad n = 0, 1, \dots, K. \quad (29)$$

The by-product of this analysis is that, assuming (27), the explicit form of bounds and constants such as  $\mu_j$ ,  $\delta$ ,  $\nu$  are derived and  $\tilde{C} = \frac{C_1}{C_0} = \max_{j=1, \dots, m} \exp(\mu_j x_{N-1})$ . The grid size  $\Delta x, \Delta t$  is not fixed and can be chosen arbitrarily provided that the CFL condition is satisfied.

**Remark 4.4.** *One observes that the presented result is weaker than the corresponding continuous result obtained in [28, Theorem 2.3]. Therein, no assumption on the boundedness of  $T$  is required. The continuous Lyapunov function can be shown to be equivalent to the  $H^2$ -norm of  $u$ . The exponential decay of this Lyapunov function therefore yields the global existence of  $u$ .*

A simple linear transport is considered [6]:

$$\frac{\partial}{\partial t} \begin{pmatrix} u_1 \\ u_2 \end{pmatrix} + \frac{\partial}{\partial x} \begin{pmatrix} 1 & 0 \\ 0 & -1 \end{pmatrix} \begin{pmatrix} u_1 \\ u_2 \end{pmatrix} = 0, \quad x \in [0, 1], t \in [0, T] \quad (30)$$

and subject to the boundary and initial conditions

$$u_1(t, 0) = \kappa u_2(t, 0), \quad u_2(t, 1) = \kappa u_1(t, 1), \quad u_i(0, x) = u_i^0. \quad (31)$$

In this example, the analytical decay rates  $\nu$  of the Lyapunov function is of interest. In the following numerical computations, a three point scheme given above is used in each component as in Equation (25). A time horizon fixed at  $T = 12$  is taken and constant initial data  $u_1^0 = -\frac{1}{2}$  and  $u_2^0 = \frac{1}{2}$  are prescribed. The value of the Lyapunov function is computed by  $L_n^{\text{exact}} := L^0 \exp(-\nu t^n)$  with  $\nu$ . These values are compared to those of the numerical Lyapunov function  $L^n$ . The  $L^2$ - and  $L^\infty$ -difference between both for different choices of the computational grid, boundary damping  $\kappa$  and values of the CFL constant are considered.

The parameter is fixed at  $\kappa = \frac{3}{4}$  and the sharpest possible bound is set for the CFL constant,  $\text{CFL} = 1$ . In Table 1, the results for different grid sizes  $\Delta x = \frac{1}{N}$  are presented. In the  $L^2$  and  $L^{\text{inf}}$  the expected first-order convergence of the numerical discretisation is observed. Further, the values of  $\mu$  and  $\nu$  also converge towards the theoretical value in the case  $\Delta x \rightarrow 0$  which are given by  $\mu = \ln \kappa^{-2} = 5.75\text{E-}01$  and  $\nu = \mu$ .



Table 1: The number of cells in the spatial domain  $[0, 1]$  is denoted by  $N$ .  $L^{\text{inf}}$  denotes the norm  $\|(L_n^{\text{exact}})_n - (L^n)_n\|_{\infty}$  and  $L^2$  the norm  $\|(L_n^{\text{exact}})_n - (L^n)_n\|_2$ . The CFL constant is equal to one and  $\kappa = \frac{3}{4}$  [6].

$N$	$L^{\text{inf}}$	$L^2$	$\mu$	$\nu$
100	4.32E-03	7.48E-04	5.66E-01	5.69E-01
200	2.18E-03	2.67E-04	5.70E-01	5.72E-01
400	1.09E-03	9.49E-05	5.73E-01	5.73E-01
800	5.48E-04	3.36E-05	5.74E-01	5.74E-01
1600	2.74E-05	1.19E-05	5.75E-01	5.75E-01

## 5 Summary

In this discussion, it has been shown that modelling in networked flow is developed by integrating a variety of existing models. This process is a multi-disciplinary process. Coupling conditions for the isothermal Euler equations in the case of multiple pipe connections were introduced. Results on existence of solutions at a pipe-to-pipe intersection have been highlighted. Numerical results were also presented which demonstrate a resolution of a shock wave. Optimal control of compressors was also discussed. Lastly, a discussion on boundary stabilisation of flow was also presented. Indeed, mathematics can be treated as a key technology which can help understand details of real-world problems for research and design.

This field is still very active as evidenced by different applications, publications as well as journals which have come into existence in the recent past. See also [32] for recent developments. It is hoped that those interested in doing mathematics with a direct link to real-world problems will join us in doing mathematics of fluid flow on networks.

## References

- [1] L. Euler, 1736, Solutio Problematis ad Geometriam Situs Pertinentis, *Commentarii Academiae Scientiarum Imperialis Petropolitanae*, 8, 128–40.
- [2] D.J. Watts & S.H. Strogatz, 1998, Collective dynamics of “small-world” networks, *Nature*, 393, 440–442.
- [3] M.E.J. Newman, The structure and function of complex networks, *SIAM Rev.*, 45(2), 167 – 256.
- [4] M. K. Banda, M. Herty & A. Klar, 2006, Coupling conditions for gas network governed by the isothermal Euler equations, *Netw. Heterog. Media*, 1, 295–314.
- [5] M. K. Banda & M. Herty, 2011, Towards a space-mapping approach to dynamic compressor optimization of gas networks, *Optimal Control Appl. and Meth.*, 32(3), 253–269.
- [6] M. K. Banda & M. Herty, 2013, Numerical discretization of stabilization problems with boundary controls for systems of hyperbolic conservation laws, *Math. Contr. Relat. Fields*, 3(2), 121–142.
- [7] M. K. Banda, M. Herty & A. Klar, 2006, Gas flow in pipeline Networks, *Netw. Heterog. Media*, 1, 41–56.
- [8] A. Martin and M. Möller & S. Moritz, 2006, Mixed integer models for the stationary case of gas network optimization, *Math. Program.*, Ser. B, 105, 563–582.
- [9] K. Ehrhardt & M. Steinbach, 2005, Nonlinear gas optimization in gas networks, in H. G. Bock, E. Kostina, H. X. Pu, R. Rannacher (eds), *Modeling, simulation and optimization of complex processes*, Springer Verlag, Berlin.
- [10] M. Steinbach, 2007 On PDE Solution in transient optimization of gas networks, *J. Comput. Appl. Math.*, 203(2), 345–361.
- [11] J. Zhou & M. A. Adewumi, 2000, Simulation of transients in natural gas pipelines using hybrid TVD schemes, *Int. J. Numer. Meth. Fluids*, 32, 407–437.
- [12] N.H. Chen, 1979, An explicit equation for friction factor in pipe, *Ind. Eng. Chem. Fund.*, 18, 296–297.
- [13] R. J. LeVeque, 1992, *Numerical methods for conservation laws*, Birkhäuser Verlag, Boston.
- [14] C. M. Dafermos, 2005, *Hyperbolic conservation laws in continuum physics*, 2<sup>nd</sup> ed., Springer, New York.
- [15] M. Gugat, M. Herty, A. Klar, G. Leugering & V. Schleper, 2012, Well-posedness of networked hyperbolic systems of balance laws, *Int. Ser. of Num. Math.*, 160, 123–146.
- [16] F. M. White, 2002, *Fluid Mechanics*, McGraw–Hill, New York.
- [17] Crane Valve Group, 1998, *Flow of fluids through valves, fittings and pipes*, Crane Technical Paper No. 410.
- [18] R. M. Colombo & M. Garavello, 2006, A well-posed Riemann problem for the p-system at a junction, *Netw. Heterog. Media*, 1, 495–511.
- [19] A. Bressan, 2005, *Hyperbolic systems of conservation laws: The one-dimensional Cauchy problem*, Oxford Lecture Series in Mathematics and its applications, 20, Oxford University Press.
- [20] M. Herty and M. Rascle, 2006, Coupling conditions for a class of second order models for traffic flow, *SIAM J. Math. Anal.*, 38, 592–616.
- [21] M.K. Banda, M. Herty, & J.-M. T. Ngnotchouye, 2010, Towards a mathematical analysis for drift-flux multiphase flow models in networks, *SIAM J. Sci. Comput.*, 31(6), 4633 – 4653.

- [22] M. K. Banda & M. Herty, 2008, Multiscale modelling for gas flow in pipe networks, *Math. Meth. Appl. Sc.*, 31(8), 915–936.
- [23] A. Bressan & G. Guerra, 1997, Shift-differentiability of the flow generated by a conservative law, *Discr. Contin. Dynam. Sys.*, 3, 35–58.
- [24] S. Bianchini, 2000, On the shift-differentiability of the flow generated by a hyperbolic system of conservative laws, *Discrete Contin. Dynam. Sys.*, 6, 329–350.
- [25] S. Ulbrich, 2003, Adjoint-based derivative computations for the optimal control of discontinuous solutions of hyperbolic conservation laws, *System and Control Letters*, 3, 309.
- [26] D. Echeverria & P. W. Hemker, 2005, Space mapping and defect correction, *Comput. Methods Appl. Math.*, 5, 107–136.
- [27] J.W. Bandler, R.M. Biernacki, S.H. Chen, P.A. Grobelny & R.H. Hemmers, 1994, Space mapping technique for electromagnetic optimization, *IEEE Trans. Microwave Theory Tech.*, 42, 2536–2544.
- [28] J.-M. Coron, G. Bastin & B. d’Andréa-Novel, 2008, Dissipative boundary conditions for one-dimensional nonlinear hyperbolic systems, *SIAM J. Control. Optim.*, 47, 1460–1498.
- [29] J.-M. Coron, 2002, Local controllability of a 1-D tank containing a fluid modelled by the shallow water equations, *ESAIM:COCV*, 8, 513–554.
- [30] J.-M. Coron, 2007, Control and Nonlinearity, *Mathematical Surveys and Monographs*, 136, American Mathematical Society, Providence, RI.
- [31] T. Li, B. Rao & Z. Wang, 2008, Contrôlabilité observabilité unilatérales de systèmes hyperboliques quasi-linéaires, *C. R. Math. Acad. Sci. Paris*, 346, 1067–1072.
- [32] Pipeline Simulation Interest Group, [www.psig.org](http://www.psig.org).